Supplement of Atmos. Chem. Phys., 18, 17843–17861, 2018
https://doi.org/10.5194/acp-18-17843-2018-supplement

Atmospheric Chemistry and Physics
Open Access
EGU

Supplement of

Production of particulate brown carbon during atmospheric aging of residential wood-burning emissions

Nivedita K. Kumar et al.

Correspondence to: Imad El-Haddad (imad.el-haddad@psi.ch) and André S. H. Prévôt (andre.prevot@psi.ch)

S1 Wall loss correction

Solving the equations in Section 3.1 requires the determination of the time-dependent concentrations of the different absorbing species, which may be governed by their photochemical production or decay as well as by diffusion, electrostatic and gravitational losses to the walls. Assuming all particles are equally lost to the walls, an inert, non-volatile species, *X*, follows a first order decay:

$$X(t) = X(t_0) \cdot \exp(\tau^{-1}(t - t_0) \quad \text{(S1)}$$

Here, t and t_0 denote the time of interest and reference time, respectively. The time constant τ is the lifetime of *X* with respect to particle wall losses. We determined τ by fitting $b_{abs}(t, 880nm)$ to Equation S1. Only the last period of each experiment was chosen for fitting, when secondary organic aerosol production rates are smaller. On average, τ equals 3.9±0.8 hours for our chamber. The wall loss corrected absorption coefficient, $b_{abs}^{WLC}(t, 880\,nm)$, varied less than 8% throughout the experiment, with higher values in the first period of measurements. Therefore we conclude that the first order decay is an appropriate approach for the wall loss correction of inert particulate properties. We ascribe the residual variations of $b_{abs}^{WLC}(t, 880\,nm)$ to a combination of uncertainties, including the aethalometer compensation parameter and possible small changes of MAC_{BC}(880nm) with aging.

For the extrapolation of our data to ambient environments we computed the average SOA mass formed as a function of OH exposure during the different experiments. This step requires the correction of OA mass for particle wall losses, which has been achieved by assuming two cases: (1) condensable oxidized gases do not interact with wall-deposited particles and (2) condensable oxidized gases condense at similar rates onto the suspended and wall-deposited particles (Pierce et al., 2008). We did not consider the deposition of oxidized vapors onto the clean Teflon walls, which would require knowledge of the saturation vapor pressures of the compounds, the condensed phase bulk properties and the vapor-wall equilibration rates. It is likely that the large particle condensational sinks utilized here (with a particle surface area concentration of several hundreds of μm^2 cm^{-3}), outcompeted vapor deposition onto the walls. Therefore, we consider the vapor deposition to the clean Teflon wall to be of a minor importance compared to burn-to-burn variability and other experimental uncertainties.

Solving the mass balance equations of the suspended organic aerosol, $[OA_{sus}(t)]$, and the organic aerosol on the walls yields the expressions in Equations (S2) and (S3), when considering scenario (1) and (2), respectively:

$$\left[M_{OA,wlc,1}(t)\right]=\left[M_{OA,sus}(t)\right]+\int_0^t \tau^{-1}\left[M_{OA,sus}(t)\right]dt \quad \text{(S2)}$$

$$\left[M_{OA,wlc,2}(t)\right]=\left[M_{OA,sus}(t)\right]*\exp(\tau^{-1}t) \quad \text{(S3)}$$

Here, $[M_{OA,wlc}(t)]$ is the wall-loss-corrected OA concentration. The results presented in Fig. 8 in the manuscript are the average time-series of all experiments considering both scenarios, and associated ranges entail both the experiment-to-experiment variability and the uncertainties related to wall loss corrections.

Supplementary figures

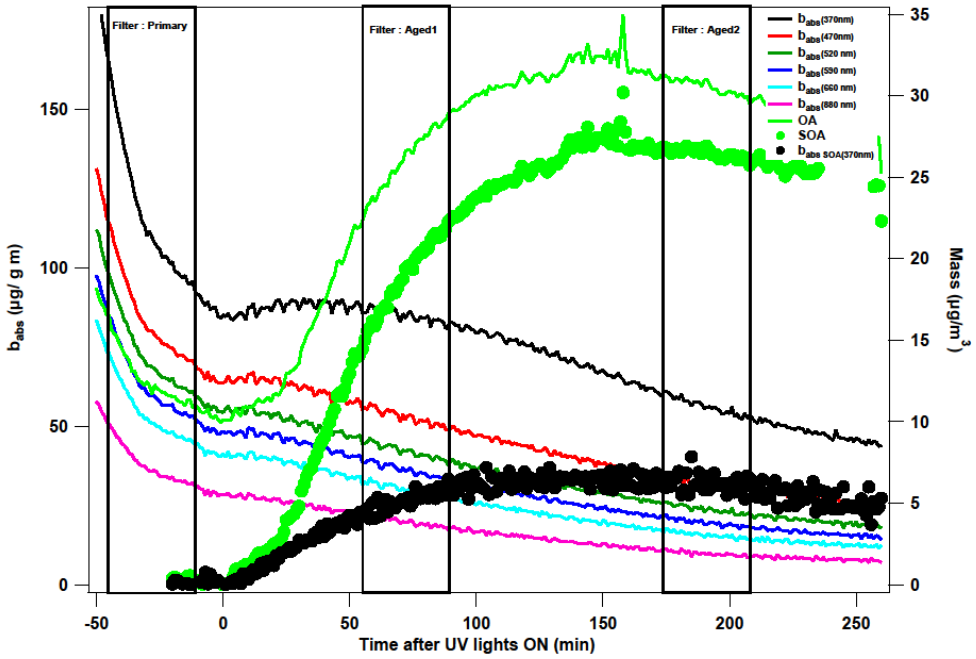

Figure S1: Absorption coefficients of fresh and aged emissions measured at 6 different wavelengths (i.e. 370 – 880 nm) using the aethalometer. The OA is measured using an AMS. Dotted lines are primary-subtracted OA (SOA) and absorption coefficient (b_{absSOA}(370nm)) . The black boxes mark the times where the primary, slightly aged (Aged1, OH exposure ~1x10^{7}molecules cm^{-3} h) and heavily aged filters (Aged2, OH exposure ~ 4x10^7 molecules cm^{-3} h) were collected.

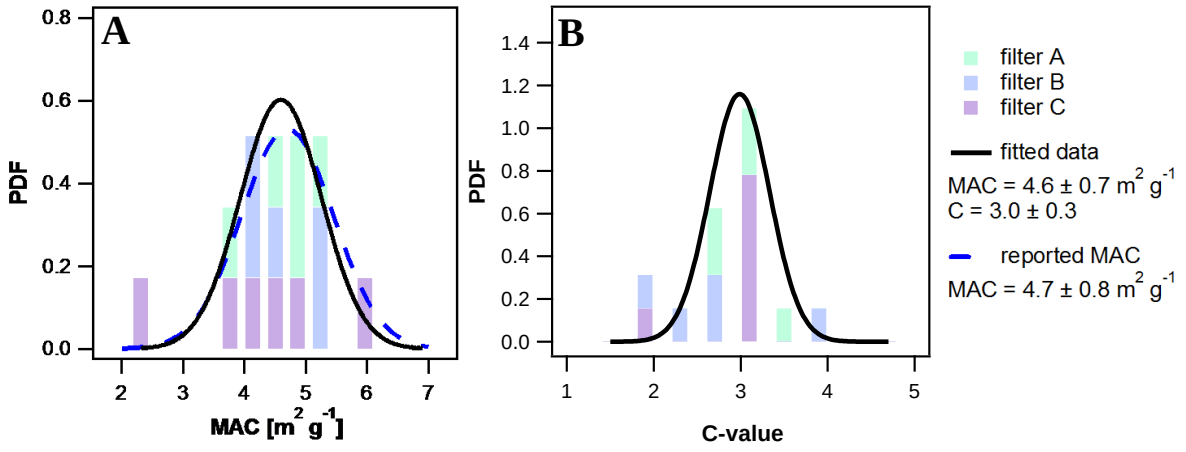

Figure S2: (a) Probability density function (PDF) comparing the MAC values determined by normalizing MWAA absorption measurements of offline primary (filter A), slightly aged (filter B: Aged1) and aged filter (filter C: Aged2) samples to EC (EUSAAR2) measurements of the same samples (bold line). A literature value for pure BC is also shown (Bond et al., 2006) (dashed blue line). (b) PDF comparing aethalometer attenutation measurements at 880 nm and MWAA absorption measurements at 850 nm to retrieve the aethalometer *C* value.

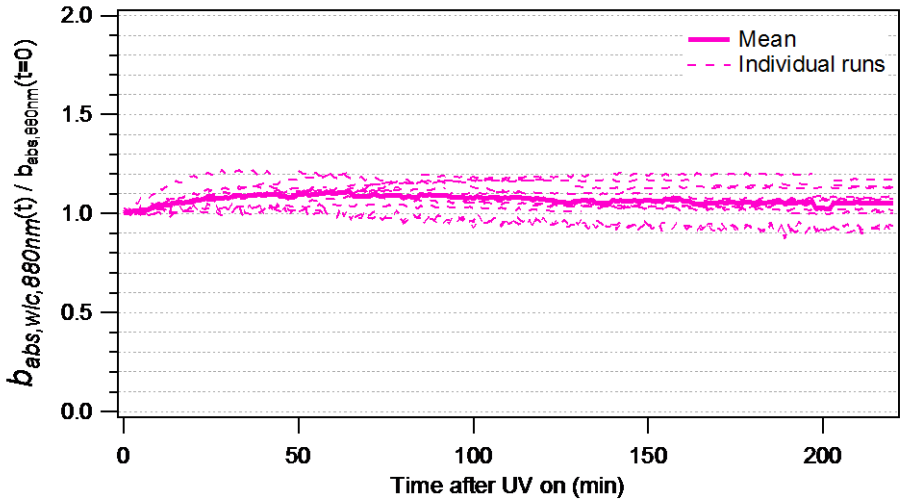

Figure S3: Wall-loss-corrected aethalometer absorption coefficient at 880 nm normalized to start-of-experiment absorption. The lack of any trend in this plot illustrates that the wall loss correction is appropriate and that only a negligible absorption increase occurs due to additional lensing by SOA.

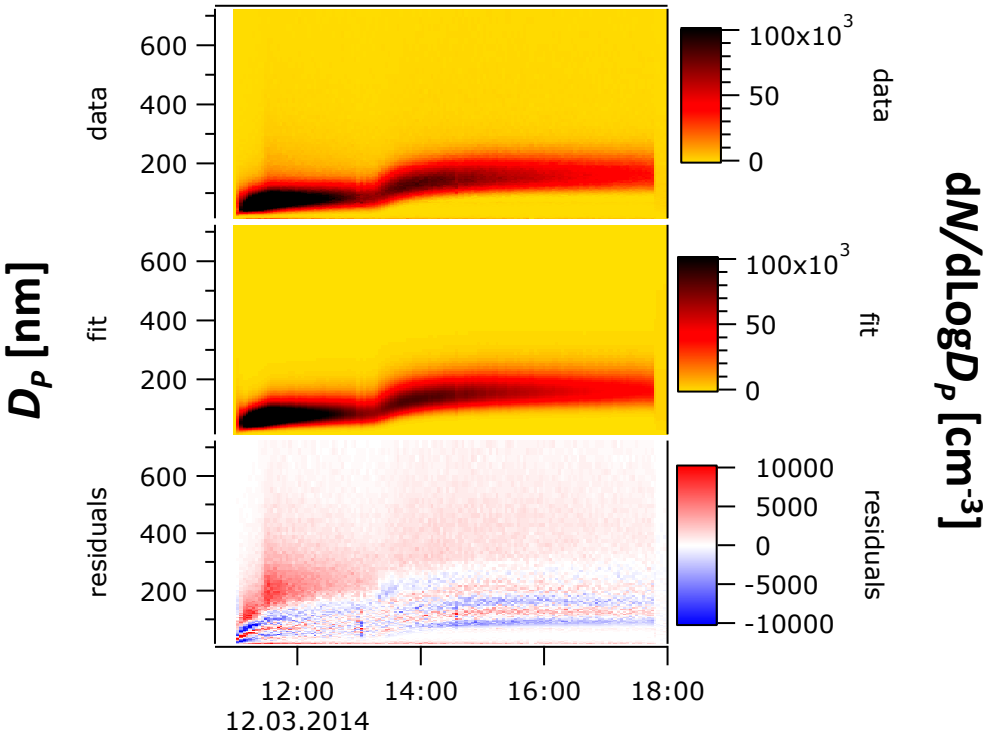

Figure S4: SMPS measurements (top), lognormal fits (middle; f_{POA}=0.51), and fit residuals (bottom) of the size distribution of biomass burning organic aerosol during a typical aging experiment.

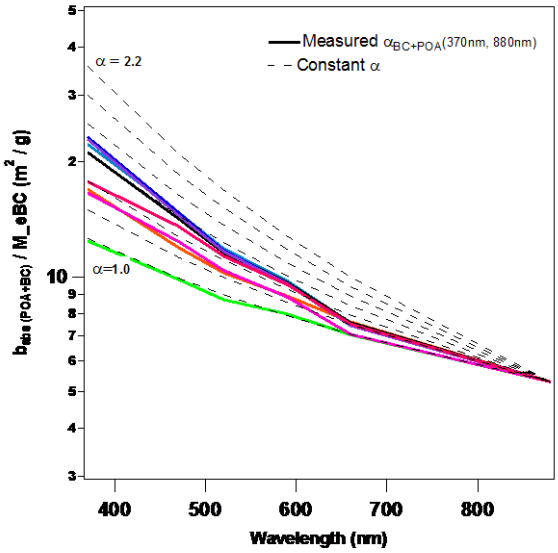

Figure S5: Absorption coefficients of fresh wood burning emissions measured using an aethalometer normalized to the eBC mass as a function of wavelength. In the legend each color denotes the α_{BC+POA}(370nm,880nm) for an individual experiment. The dashed lines mark the absorption profiles calculated assuming a constant α_{BC+POA} in the range 370-880nm. The range of α values, is set between 1-2.2 (with an increment of 0.2), based on literature reports for primary biomass burning emissions from residential heating. The observed absorption spectra have steeper gradients with decreasing wavelength compared to the lines of constant alpha. This systematic decrease in $\alpha(\lambda, 880nm)$ with increasing λ reflects the more-efficient light absorption by BrC at shorter wavelengths (Moosmüller et al., 2011), and shows that the power law wavelength dependence is an inaccurate oversimplification for this mixed aerosol.

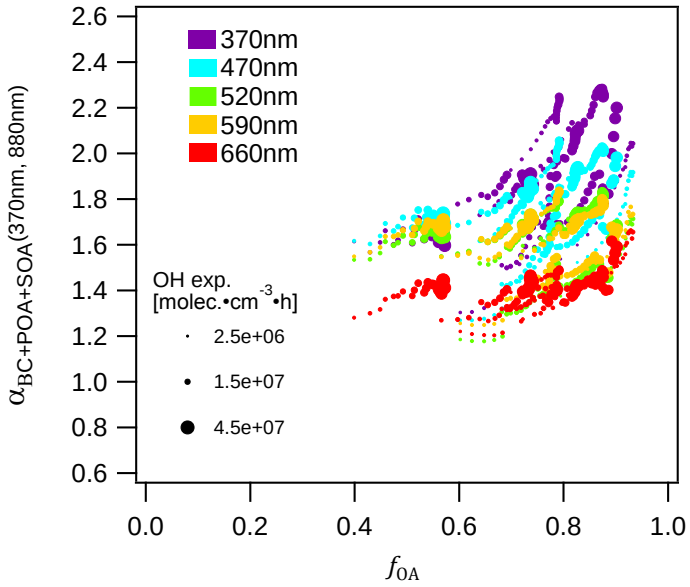

Figure S6: Relationship of $\alpha_{BC+POA+SOA}(\lambda, 880nm)$ to f_{OA} for seven wavelengths, with symbol sizes indicating OH exposure.

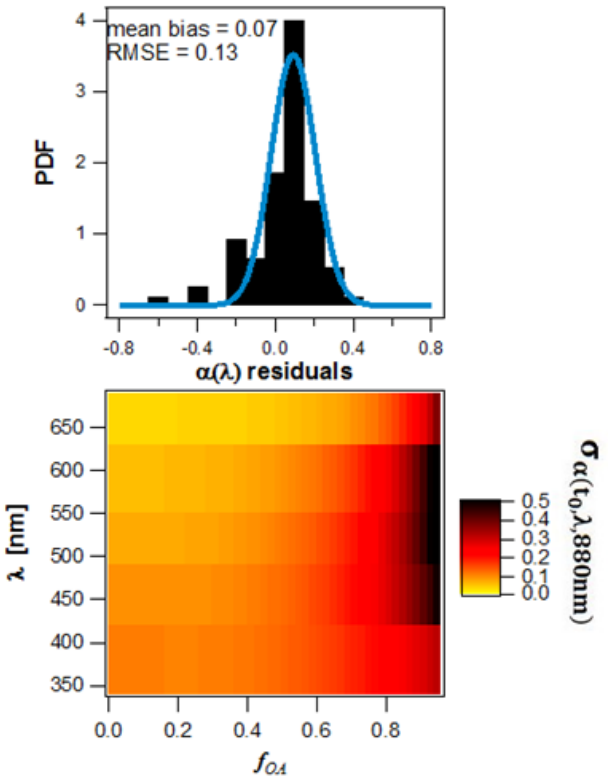

Figure S7: Analysis of the fitting errors of $\alpha(\lambda, 880nm)$ of primary emissions as a function of f_{OA}. Panel A shows the α residual as a probability density function. Panel B is an image plot of the $\alpha(\lambda, 880nm)$ error, $\sigma_{\alpha(t_0,\lambda,880nm)}$, as a function of f_{OA} at different wavelengths. $\sigma_{\alpha(t_0,\lambda,880nm)}$ is obtained from the error propagation of Eq. (13) solved for different wavelengths, using the geometric mean and standard deviation of $MAC_{POA}(\lambda)$ and $MAC_{BC}(\lambda)$. This error term represents the variability in or the confidence level on the $\alpha(t_0, \lambda, 880nm)$ at different wavelengths. As $\alpha(t_0, \lambda, 880nm)$ depends on $M_{OA}/ b_{abs}(t_0, 880nm)$ in Equation 13, $\sigma_{\alpha(t_0,\lambda,880nm)}$ also does. We expressed $M_{OA}/b_{abs}(t_0, 880nm)$ as f_{OA}, using σ_{ATN} to estimate EC mass from b_{ATN}(880nm). At short wavelengths and low OA fractions, the confidence level on α is within 0.1. However, with increasing f_{OA}, and at longer wavelength the uncertainty in predicting α increases.

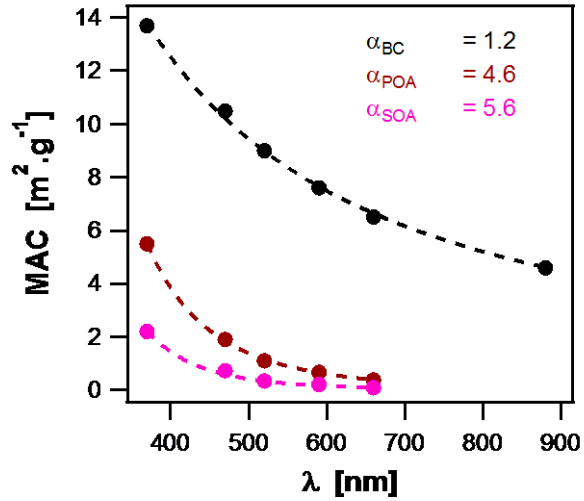

Figure S8: Power law fits through the average MAC of BC, POA and SOA calculated from Aethalometer measurements plotted as a function of wavelength. Note that MAC_{SOA}(880nm) and MAC_{POA}(880nm) are zero by definition.

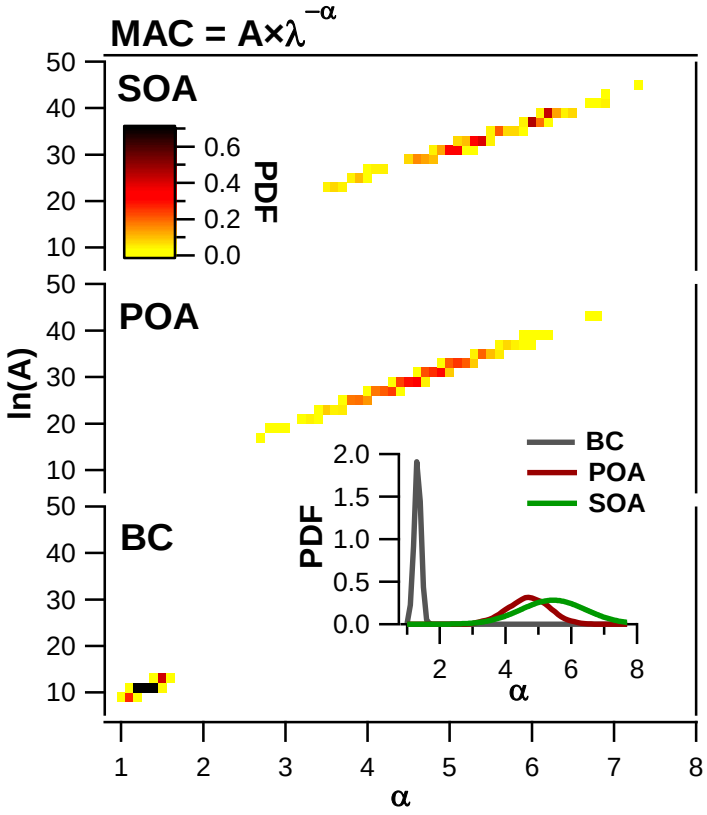

Figure S9: Probability distributions of α and ln(A) describing the optical properties of BC, POA and SOA. Parameters for representing these distributions as a bivariate normal joint density function are shown in Table S1. The equation needed to generate these probabilities is $f(\mathbf{X}) = \frac{|\Sigma|^{-\frac{1}{2}}}{2\pi} \exp\left(-\frac{1}{2}(\mathbf{X}-\mu)^{\mathrm{T}}\Sigma^{-1}(\mathbf{X}-\mu)\right)$**, where** $\mu = \begin{pmatrix} \mu_{\alpha} \\ \mu_{\ln(A)} \end{pmatrix}$**; represents the average α and ln(A) values and** $\Sigma = \begin{pmatrix} \sigma_{\alpha}^2 & \rho\sigma_{\alpha}\sigma_{\ln(A)} \\ \rho\sigma_{\alpha}\sigma_{\ln(A)} & \sigma_{\ln(A)}^2 \end{pmatrix}$ **is the covariance matrix. As α and ln(A) are determined from fitting the MAC vs. λ, their covariance is high. Therefore the selection of these parameters to represent the MAC profiles of BC, POA and SOA, should not be done independently but by using the probability density function above and the parameters in Table S1.**

Table S1: Parameters for normal joint density function.

	BC	**POA**	**SOA**
μ	$\begin{pmatrix} 1.2 \\ 10.0 \end{pmatrix}$	$\begin{pmatrix} 4.6 \\ 29.2 \end{pmatrix}$	$\begin{pmatrix} 5.6 \\ 33.3 \end{pmatrix}$
Σ	$\begin{pmatrix} 0.09 & 0.054 \\ 0.054 & 0.61 \end{pmatrix}$	$\begin{pmatrix} 0.64 & 2.6 \\ 2.6 & 4.1 \end{pmatrix}$	$\begin{pmatrix} 1.36 & 11.4 \\ 11.4 & 8.35 \end{pmatrix}$

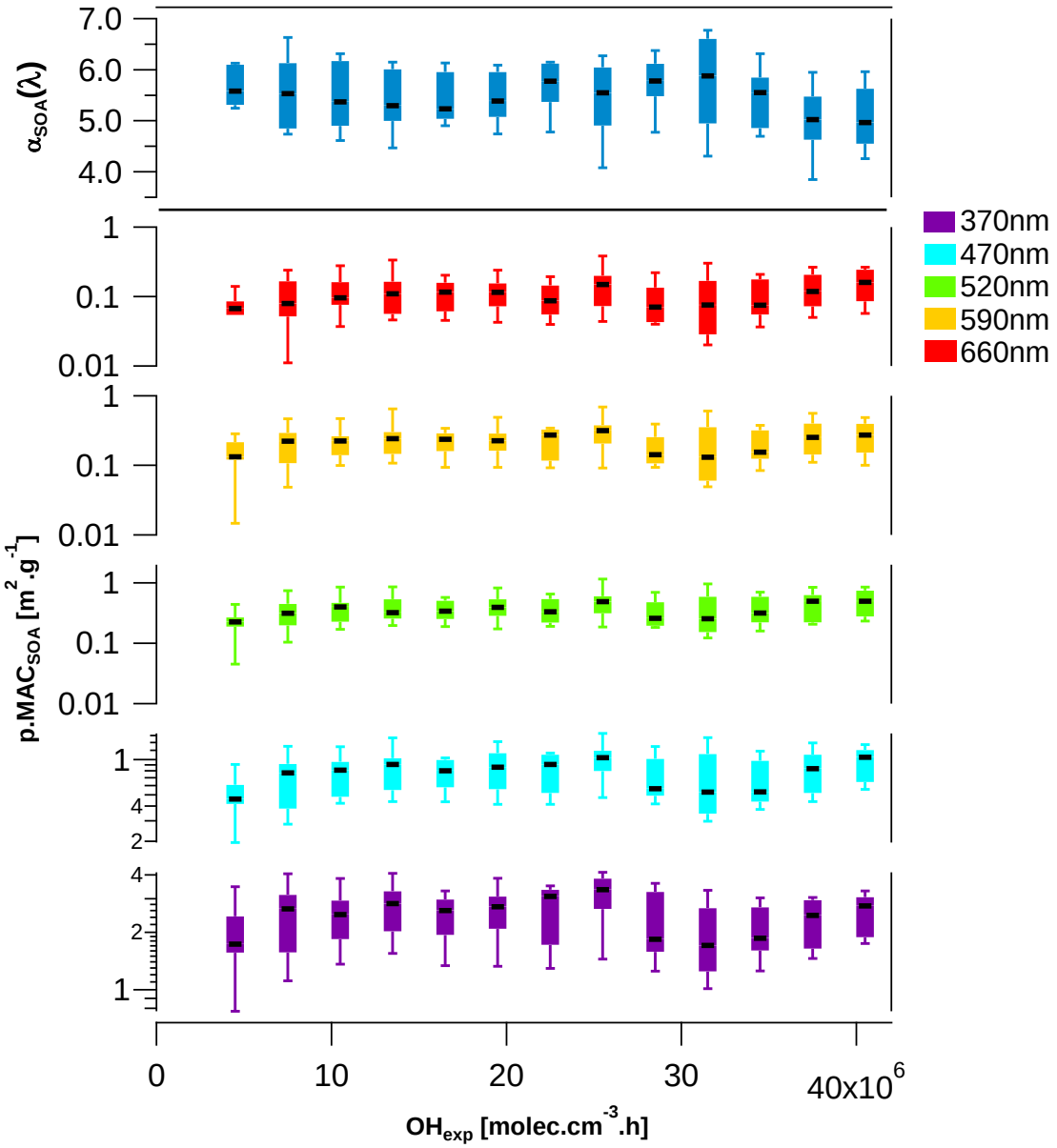

Figure S10: MAC_{SOA} as a function of OH exposure color coded according to the wavelength.

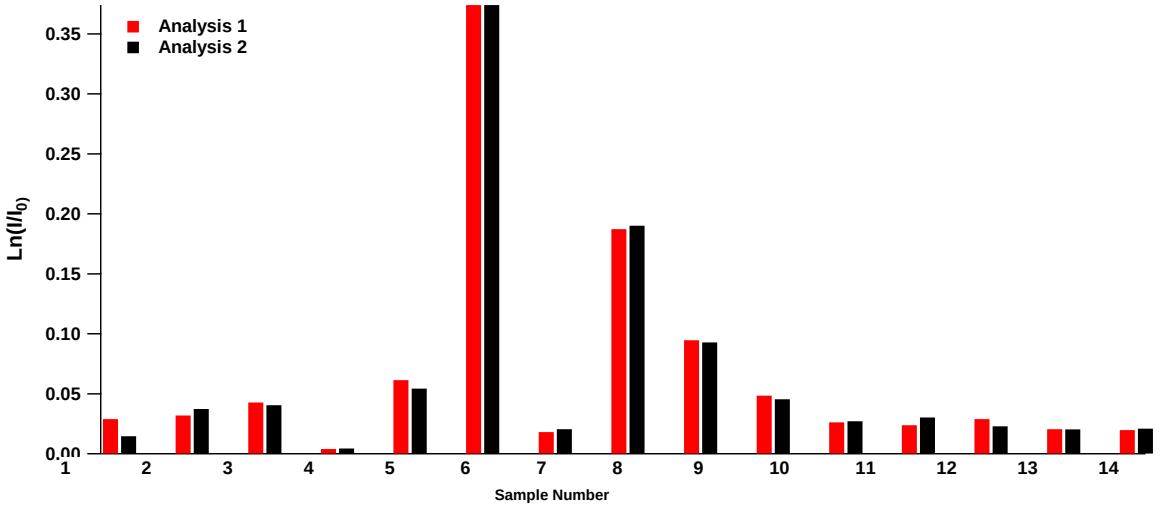

Figure S11: Absorbance measurements from UV-visible analysis of water extracted filters from several wood burning experiments showing very good repeatability (consistent within 10%).

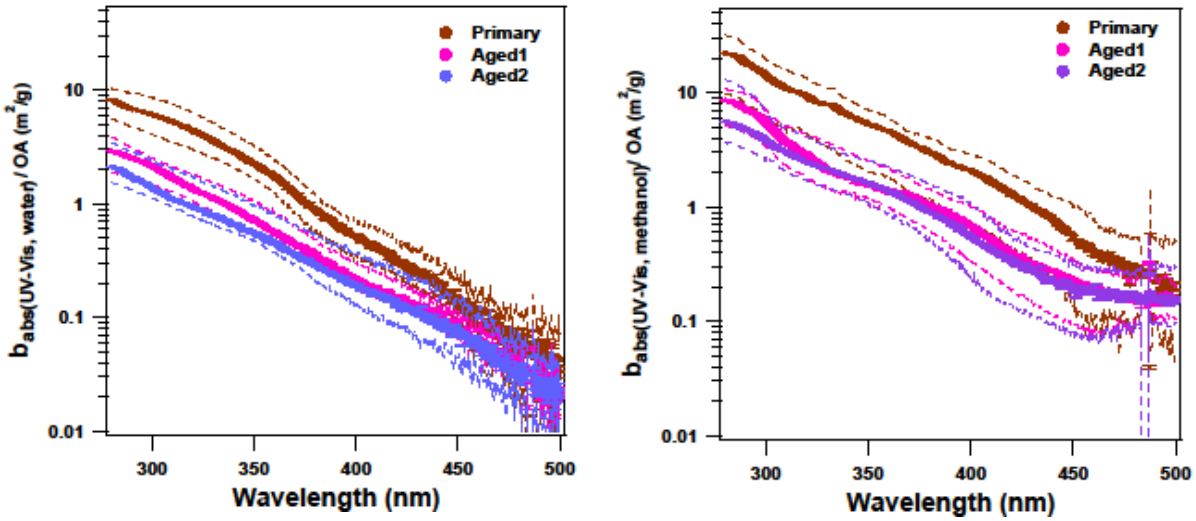

Figure S12: MAC_{bulk} (bulk absorbance of extracts normalized to AMS-measured OA) of primary, slightly aged (Aged1, OH exposure ~ $1x10^7$molecules cm^{-3} h) and aged emissions (Aged2, OH exposure ~ $4x10^7$ molecules cm^{-3} h) for (A) water and (B) methanol extracts. The bold lines indicate the medians, and the dashed lines mark the 25th and 75th percentiles. At 450–500 nm, the methanol-extract absorption shows a constant absorptivity feature which was not present before aging, suggesting that the absorbing species may be partially-oxidized (partially-solubilized) primary OA, or reflect light-absorbing SOA.

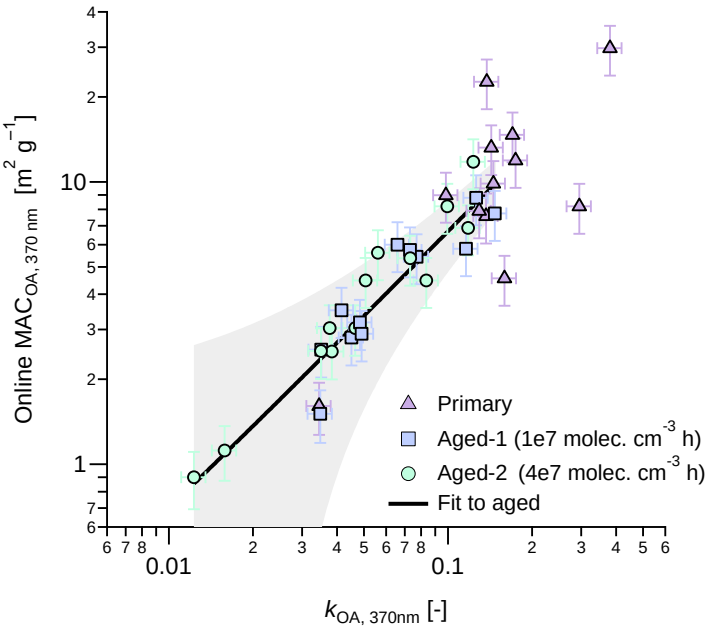

Figure S13: MAC$_{OA}$ at λ = 370 nm calculated from aethalometer measurements vs. k$_{OA}$ at λ = 370 nm from the UV/visible measurements of the methanol extracts. The shaded region shows the 90% confidence interval of a weighted orthogonal regression (slope 66 ± 9 m^{2}g^{-1}, intercept 0.0 ± 0.3 m^{2}g^{-1}) to illustrate the relatively small range of variability in the data for aged samples.

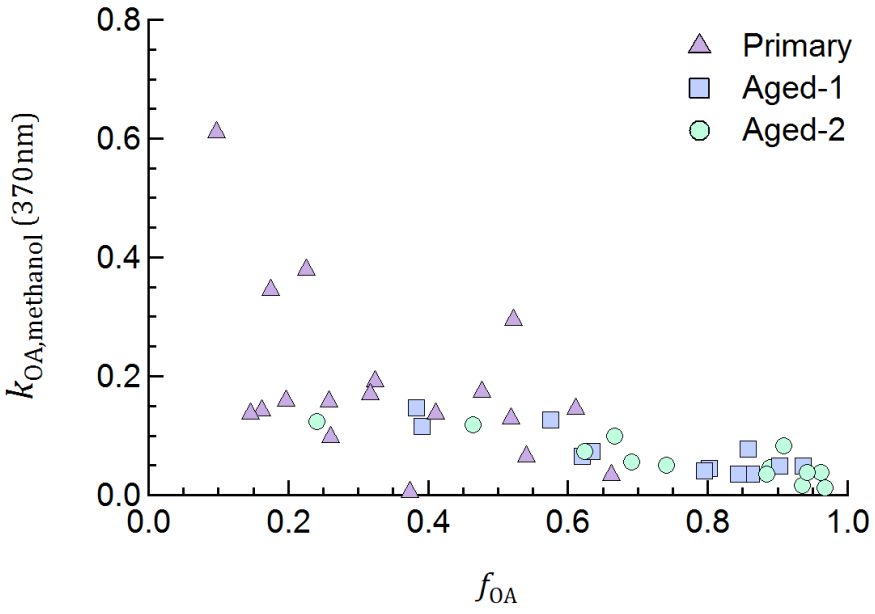

Figure S14. Similar to Fig. 7 in the main text, but plotted against f_{OA} for comparison to the other figures in this work.

References

Pierce, J. R., Engelhart, G. J., Hildebrandt, L., Weitkamp, E. A., Pathak, R. K., Donahue, N. M., Robinson, A. L., Adams, P. J. and Pandis, S. N.: Constraining particle evolution from wall losses, coagulation, and condensation-evaporation in smog-chamber experiments: optimal estimation based on size distribution measurements, Aerosol Sci. Technol., 42, 1001–1015, doi:10.1080/02786820802389251, 2008.

Bond, T. C., Habib, G. and Bergstrom, R. W.: Limitations in the enhancement of visible light absorption due to

mixing state, J. Geophys. Res. Atmos., 111(20), 1–13, doi:10.1029/2006JD007315, 2006.